CCI+ PHASE 1 – NEW ECVS
PERMAFROST

D4.3 PRODUCT USER GUIDE (PUG)

VERSION 4.0

15 FEBRUARY 2024

PREPARED BY

b·geos
GAMMA REMOTE SENSING
UiO University of Oslo
AWI
UNI FR UNIVERSITÉ DE FRIBOURG UNIVERSITÄT FREIBURG
Stockholm University
West University of Timisoara
TERRASIGNA

Document Status Sheet

Issue	Date	Details	Authors
1.0	30.09.2019	Completion of v1	A. Bartsch (B.GEOS), J. Obu (University of Oslo)
1.1	18.10.2019	Update of 'known limitations' with respect to PVIR v1	S. Westermann (University of Oslo), A. Bartsch (B.GEOS)
2.0	31.05.2020	Update for year 2 data	A. Bartsch (B.GEOS), S. Westermann (Univ. Oslo)
2.1	20.10.2020	Meta data description update (file naming), known issues update based on CAR, GlobPermafrost legacy inclusion	A. Bartsch (B.GEOS), S. Westermann (University of Oslo)
2.2	02.02.2021	Source for Yedoma spatial information added, Section 'known issues'	A. Bartsch (B.GEOS)
3.0	13.04.2021	Update for year 3 data (version ID, temporal extension, known issues)	A. Bartsch (B.GEOS)
4.0	15.02.2024	Update for first iteration of Phase II (version ID, temporal extension, known issues, CMUG feedback)	A. Bartsch (B.GEOS)

Author team

Annett Bartsch, B.GEOS

Jaroslav Obu, University of Oslo

Sebastian Westermann, University of Oslo

Tazio Strozzi, GAMMA

ESA Technical Officer:
Frank Martin Seifert

Contact for questions and feedback: annett.bartsch@bgeos.com

TABLE OF CONTENTS

EXECUTIVE SUMMARY

Within the European Space Agency (ESA), the Climate Change Initiative (CCI) is a global monitoring program which aims to provide long-term satellite-based products to serve the climate modeling and climate user community. Permafrost has been selected as one of the Essential Climate Variables (ECVs) which are elaborated during Phase 1 of CCI+ (2018-2021) and continued during Phase 2 of CCI+ (2022-2025).

The PUG provides the description of the Climate Research Data Package (CRDP). This includes formats, attributes and meta data. The CRDP includes the ECV state variables ground temperature and active layer thickness, derived from a thermal model driven and constrained by EO data. In addition, the product provides a yearly fraction of permafrost-underlain and permafrost-free area within a pixel.

CRDPv3 covers the years from 1997 to 2021, with the data available for each year of the period. It covers Arctic and High-Mountain permafrost environments of the northern hemisphere. The projection is geographic, with 0.01° grid spacing conform with LST_cci and Snow_cci datasets. It is provided in NetCDF format including meta data following the NetCDF Climate and Forecast (CF) Metadata Convention 73.

Known limitations include regional biases and specifically shortcomings of input stratigraphy.

1 INTRODUCTION

1.1 Purpose of the document

This document provides the user requirements of climate science and climate services for ECV products of the Permafrost_cci project. The ultimate objective of Permafrost_cci is to develop and deliver permafrost maps as ECV products primarily derived from satellite measurements.

Permafrost is an Essential Climate Variable (ECV) within the Global Climate Observing System (GCOS), which is characterized by subsurface temperatures and the depth of the seasonal thaw layer. Complementing ground-based monitoring networks, the Permafrost CCI project is establishing Earth Observation (EO) based products for the permafrost ECV spanning the last two decades. Since ground temperature and thaw depth cannot be directly observed from space-borne sensors, a variety of satellite and reanalysis data are combined in a ground thermal model. The algorithm uses remotely sensed data sets of Land Surface Temperature (MODIS LST/ ESA LST CCI) and landcover (ESA Landcover CCI) to drive the transient permafrost model CryoGrid 2, which yields thaw depth and ground temperature at various depths, while ground temperature forms the basis for permafrost fraction [RD-3]. The Land Surface Temperature data sets are employed to determine the upper boundary condition of the differential equation, while its coefficients (e.g. heat capacity and thermal conductivity) are selected according to the landcover information (Westermann et al., 2017). With this, a spatial resolution of the final product of 1 km is possible, corresponding to "breakthrough" according to the WMO OSCAR database [RD-5].

The PUG provides the description of the Climate Research Data Package (CRDP). This includes formats, attributes and meta data.

The CRDP v3 includes the ECV state variables ground temperature and active layer thickness, derived from a thermal model driven and constrained by EO data. In addition, the product provides a yearly fraction of permafrost-underlain and permafrost-free area within a pixel.

1.2 Structure of the document

The first part of this document details general properties of all products. Attributes and known issues, with reference to the Product Validation and Intercomparison Report (PVIR) are described in a separate chapter. Bibliography and abbreviations are provided at the end of the document.

2 General product properties

2.1 Temporal compositing

Grid products of CDRP v3 are released in annual files, covering the start to the end of the Julian year. This corresponds to average annual ground temperatures, as well as the maximum depth of seasonal thaw, which corresponds to the active layer thickness.

2.2 Spatial resolution

The spatial resolution of the grid product is 0.01°. Grid attributes are computed in each cell of that size within the time period indicated above. The spatial resolution is limited by the spatial resolution of remotely sensed Landsurface Temperature.

2.3 Product projection system

The projection is in geographic coordinates at 0.01° resolution.

2.4 File formats, size and value range

The product is delivered in NetCDF format, with each time slice and parameter as an individual file.

Table 1: File characteristics (data values available for maximum permafrost extent in record only)

Type	**Data size per year/file**	**Minimum**	**Maximum**	**Mean (2021)**	**Standard deviation (2021)**
GTD	368.5 MB	-20°C at 2m	7°C at 2m	-3°C at 2m	5.9°C at 2m
ALT	36.3 MB	0cm	900cm	54.3cm	43.7cm
PFR	157.3 MB	0%	100%	77.41%	29.87%

2.5 Geographical subsets

CRDPv3 pertains Arctic and High-Mountain permafrost environments, extending from 85°N down to 35 °N latitude in the North America and down to 25 °N in Asia.

2.6 Product file naming conventions

The files for each product type are named as follows:

ESACCI-<CCI Project>-<Processing Level>-<Data Type>-<Product String>[-<Additional Segregator>]-<Start Date>-<End Date>-fv<File version>.nc

<CCI Project>

PERMAFROST for Permafrost_cci

<Processing Level>
L4 for Level 4; Data sets are created from the analysis of lower level data, resulting in gridded, gap-free products.

<Data Type>
GTD, when the parameter is ground temperature at a certain depth, ALT, if the parameter is active layer thickness, PFR if the parameter is permafrost extent (fraction), PFF if the parameter is permafrost-free fraction, PFT if the parameter is fraction underlain by talik and PZO if the parameter is permafrost zone.

<Product String> : <source>_<algorithm>
MODIS_ CRYOGRID or ERA5_MODISLST_BIASCORRECTED
<Source>

- MODIS - MODIS Landsurface temperature is used as the main input for the L4 production for 2003-2021 data. Sensors of auxiliary data are listed in the meta data.
- ERA5 - Downscaled and bias corrected ERA reanalyses data based on statistics of the overlap period between ERA reanalysis and MODIS LST are used for data before 2003. Sensors of auxiliary data are listed in the meta data.

<algorithm>

- CRYOGRID – data from CRYOGRID algorithm
- MODISLST_BIASCORRECTED - Downscaled and bias corrected ERA reanalyses data based on statistics of the overlap period between ERA reanalysis and MODIS LST are used for data before 2003. Sensors of auxiliary data are listed in the meta data

<Additional Segregator>
This should be AREA<TILE_NUMBER>_<Layer type>
<TILE_NUMBER>being the tile number the subset index: 1- global, 2-North America, 3-Eurasia, 4-Northern Hemisphere
<Layer type>

- PP: layer type 1, corresponding to value of the permafrost parameter.

<Start Date> and <End Date>
The identifying date for this data set:
Format is YYYYMMDD, where YYYY is the four digit year, MM is the two digit month from 01 to 12 and DD is the two digit day of the month from 01 to 31.

fv<File Version>
File version number in the form n{1,}[.n{1,}] (That is 1 or more digits followed by optional . and another 1 or more digits). The most recent version is fv04.0 (released in November 2023).

Examples:
ESACCI-PERMAFROST-L4-GTD-MODIS_CRYOGRID-AREA4_PP-2011-fv04.0.nc

ESACCI-PERMAFROST-L4-GTD-ERA5_MODISLST_BIASCORRECTED-AREA4_PP-1997-fv04.0.nc

2.7 Meta data

Meta data are included in all files following the NetCDF Climate and Forecast (CF) Metadata Convention 73 [RD-1].

3 Ground temperature

3.1 Terminology

Mean annual temperature of the ground of CRDP v3 is provided for particular depths [RD-1].
The mean annual temperature of the ground usually increases with depth below the surface. In some northern areas, however, it is not un-common to find that the mean annual ground temperature decreases in the upper 50 to 100 metres below the ground surface as a result of past changes in surface and climate conditions. Below that depth, it will increase as a result of the geothermal heat flux from the interior of the earth. The mean annual ground temperature at the depth of zero annual amplitude is often used to assess the thermal regime of the ground at various locations.
REFERENCES: von Everdingen, 1998

3.2 Abstract of data publication

This dataset contains permafrost ground temperature data produced as part of the European Space Agency's (ESA) Climate Change Initiative (CCI) Permafrost project. It forms part of the second version of their Climate Research Data Package (CRDP v3). It is derived from a thermal model driven and constrained by satellite data. Grid products of CDRP v3 are released in annual files, covering the start to the end of the Julian year. This corresponds to average annual ground temperatures and is provided for specific depths (surface, 1m, 2m, 5m , 10m).

Case A: It covers the Northern Hemisphere (north of 30°) for the period 2003-2021 based on MODIS Land Surface temperature merged with downscaled ERA5 reanalysis near-surface air temperature data.
Case B: It covers the Northern Hemisphere (north of 30°) for the period 1997-2002 based on downscaled ERA5 reanalysis near-surface air temperature data which are bias-corrected with the Case A product for the overlap period 2003-2018 using a pixel-specific statistics for each day of the year.

3.3 Pixel attributes

Layer	Attribute	Units	Data type	notes
GST	Ground surface temperature (depth 0)	Kelvin	Integer	Scaled by 100
T1m	Ground temperature at 1m depth	Kelvin	Integer	Scaled by 100
T2m	Ground temperature at 2m depth	Kelvin	Integer	Scaled by 100
T5m	Ground temperature at 5m depth	Kelvin	Integer	Scaled by 100
T10m	Ground temperature at 10m depth	Kelvin	Integer	Scaled by 100

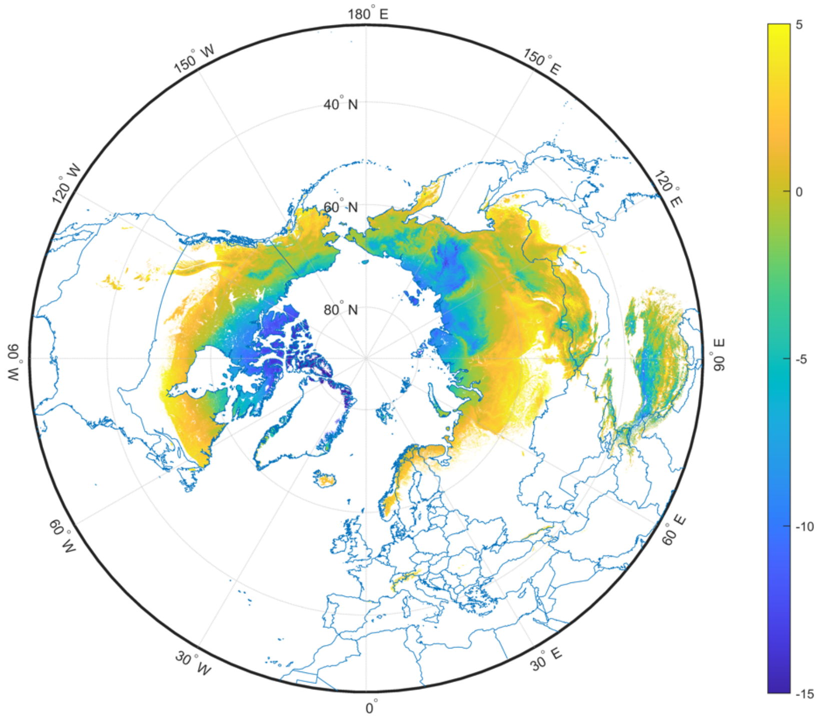

Figure 1: Example of Mean Annual Ground Temperature at 2 m depth in 2019 (in °C, colour axis).

3.4 Previous versions

ESA DUE GlobPermafrost (average for 2000-2017; equilibrium model approach; northern hemisphere, Andes, New Zealand, East African Plateau and Antarctic)

Obu, Jaroslav; Westermann, Sebastian; Kääb, Andreas; Bartsch, Annett (2018): Ground Temperature Map, 2000-2016, Northern Hemisphere Permafrost. Alfred Wegener Institute, Helmholtz Centre for Polar and Marine Research, Bremerhaven, PANGAEA, https://doi.org/10.1594/PANGAEA.888600

Obu, Jaroslav; Westermann, Sebastian; Kääb, Andreas; Bartsch, Annett (2019): Ground Temperature Map, 2000-2017, Antarctic. University of Oslo, PANGAEA, https://doi.org/10.1594/PANGAEA.902576

Obu, Jaroslav; Westermann, Sebastian; Kääb, Andreas; Bartsch, Annett (2019): Ground Temperature Map, 2000-2016, Andes, New Zealand and East African Plateau Permafrost. University of Oslo, PANGAEA, https://doi.org/10.1594/PANGAEA.905512

ESA CCI+ Permafrost_cci CRDP_v0 (file version 1 2003-2017)

Obu, J.; Westermann, S.; Barboux, C.; Bartsch, A.; Delaloye, R.; Grosse, G.; Heim, B.; Hugelius, G.; Irrgang, A.; Kääb, A.M.; Kroisleitner, C.; Matthes, H.; Nitze, I.; Pellet, C.; Seifert, F.M.; Strozzi, T.; Wegmüller, U.; Wieczorek, M.; Wiesmann, A. (2019): ESA Permafrost Climate Change Initiative (Permafrost_cci): Permafrost Ground Temperature for the Northern Hemisphere, v1.0. Centre for Environmental Data Analysis, 19 December 2019.

doi:10.5285/9a333481e9a34c7a8f78902f77ad3fe7. http://dx.doi.org/10.5285/9a333481e9a34c7a8f78902f77ad3fe7

ESA CCI+ Permafrost_cci CRDP_v1 (file version 2 1997-2018)

Obu, J.; Westermann, S.; Barboux, C.; Bartsch, A.; Delaloye, R.; Grosse, G.; Heim, B.; Hugelius, G.; Irrgang, A.; Kääb, A.M.; Kroisleitner, C.; Matthes, H.; Nitze, I.; Pellet, C.; Seifert, F.M.; Strozzi, T.; Wegmüller, U.; Wieczorek, M.; Wiesmann, A. (2020): ESA Permafrost Climate Change Initiative (Permafrost_cci): Permafrost ground temperature for the Northern Hemisphere, v2.0. Centre for Environmental Data Analysis, 02 November 2020. doi:10.5285/6ebcb73158b14cd5a321b7c0bc6ed393. http://dx.doi.org/10.5285/6ebcb73158b14cd5a321b7c0bc6ed393

ESA CCI+ Permafrost_cci CRDP_v2 (file version 3 1997-2019)

Obu, J.; Westermann, S.; Barboux, C.; Bartsch, A.; Delaloye, R.; Grosse, G.; Heim, B.; Hugelius, G.; Irrgang, A.; Kääb, A.M.; Kroisleitner, C.; Matthes, H.; Nitze, I.; Pellet, C.; Seifert, F.M.; Strozzi, T.; Wegmüller, U.; Wieczorek, M.; Wiesmann, A. (2021): ESA Permafrost Climate Change Initiative (Permafrost_cci): Permafrost Ground Temperature for the Northern Hemisphere, v3.0. NERC EDS Centre for Environmental Data Analysis, *28 June 2021*. doi:10.5285/b25d4a6174de4ac78000d034f500a268. https://dx.doi.org/10.5285/b25d4a6174de4ac78000d034f500a268

4 ACTIVE LAYER THICKNESS

4.1 Terminology

Active Layer Thickness is the thickness of the layer of the ground that is subject to annual thawing and freezing in areas underlain by permafrost.
The thickness of the active layer depends on such factors as the ambient air temperature, vegetation, drainage, soil or rock type and total water content, snowcover, and degree and orientation of slope. As a rule, the active layer is thin in the High Arctic (it can be less than 15 cm) and becomes thicker farther south (1 m or more).
The thickness of the active layer can vary from year to year, primarily due to variations in the mean annual air temperature, distribution of soil moisture, and snowcover.
The thickness of the active layer includes the uppermost part of the permafrost wherever either the salinity or clay content of the permafrost allows it to thaw and refreeze annually, even though the material remains cryotic (T < 0°C).
Use of the term "depth to permafrost" as a synonym for the thickness of the active layer is misleading, especially in areas where the active layer is separated from the permafrost by a residual thaw layer, that is, by a thawed or noncryotic (T> 0°C) layer of ground.
REFERENCES: Muller, 1943; Williams, 1965; van Everdingen, 1985.

4.2 Abstract of data publication

This dataset contains permafrost active layer thickness data produced as part of the European Space Agency's (ESA) Climate Change Initiative (CCI) Permafrost project. It forms part of the second version of their Climate Research Data Package (CRDP v3). It is derived from a thermal model driven and constrained by satellite data. Grid products of CDRP v3 are released in annual files, covering the start to the end of the Julian year. The maximum depth of seasonal thaw is provided, which corresponds to the active layer thickness.

Case A: It covers the Northern Hemisphere (north of 30°) for the period 2003-2021 based on MODIS Land Surface temperature merged with downscaled ERA5 reanalysis near-surface air temperature data.
Case B: It covers the Northern Hemisphere (north of 30°) for the period 1997-2002 based on downscaled ERA5 reanalysis near-surface air temperature data which are bias-corrected with the Case A product for the overlap period 2003-2018 using a pixel-specific statistics for each day of the year.

4.3 Pixel attributes

Layer	Attribute	Units	Data type	notes
1	Active layer thickness	meter	integer	Scaled by 100

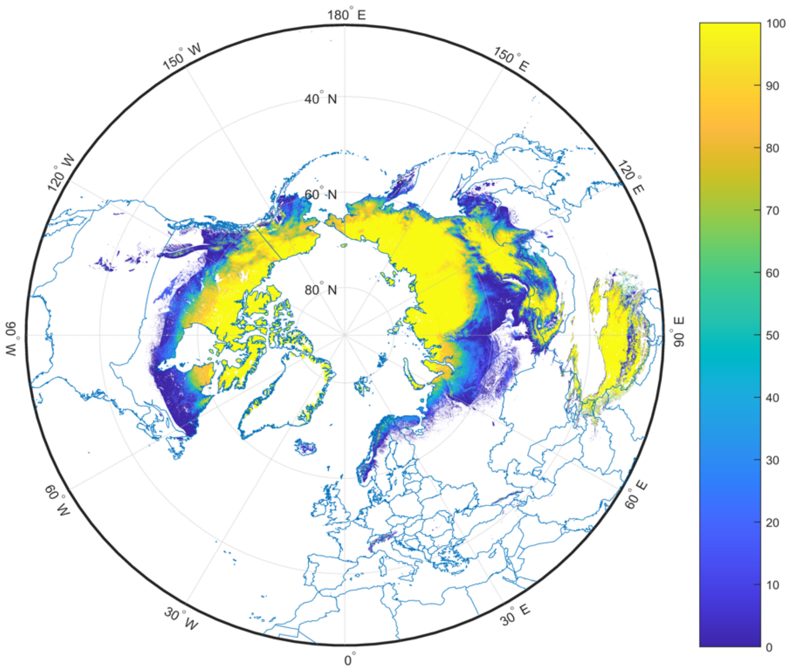

Figure 2: Example of Active Layer Thickness for 2019 (from 0 to 100%, colour axis).

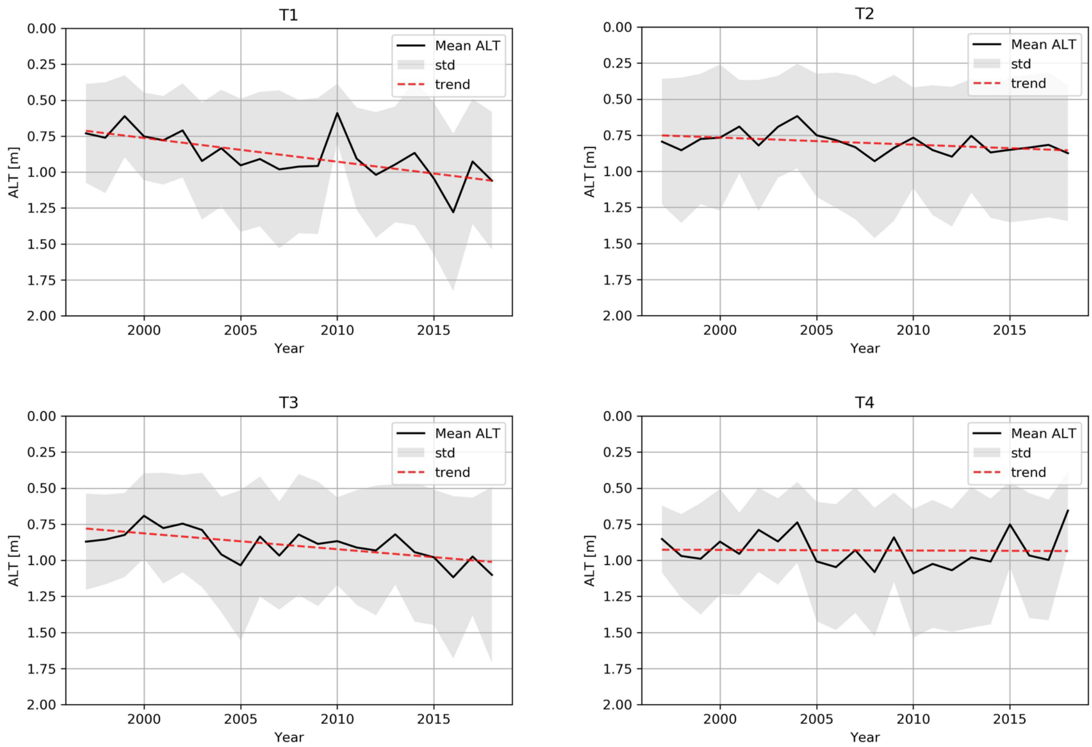

Figure 3: Comparison of Active Layer Thickness dynamics (in meter) in different HRPC Transects (T1: Western Siberia, T2: Eastern Siberia, T3: Alaska, T4: Eastern Canada) derived from annual ALT datasets (1997-2018) (source [RD-4]).

4.4 Previous version

ESA CCI+ Permafrost_cci CRDP_v0 (file version 1 2003-2017)

Obu, J.; Westermann, S.; Barboux, C.; Bartsch, A.; Delaloye, R.; Grosse, G.; Heim, B.; Hugelius, G.; Irrgang, A.; Kääb, A.M.; Kroisleitner, C.; Matthes, H.; Nitze, I.; Pellet, C.; Seifert, F.M.; Strozzi, T.; Wegmüller, U.; Wieczorek, M.; Wiesmann, A. (2019): ESA Permafrost Climate Change Initiative (Permafrost_cci): Permafrost Active Layer Thickness for the Northern Hemisphere, v1.0. Centre for Environmental Data Analysis, *19 December 2019*. doi:10.5285/1ee56c42cf6c4ef698693e00a63795f4. http://dx.doi.org/10.5285/1ee56c42cf6c4ef698693e00a63795f4

ESA CCI+ Permafrost_cci CRDP_v1 (file version 2 1997-2018)

Obu, J.; Westermann, S.; Barboux, C.; Bartsch, A.; Delaloye, R.; Grosse, G.; Heim, B.; Hugelius, G.; Irrgang, A.; Kääb, A.M.; Kroisleitner, C.; Matthes, H.; Nitze, I.; Pellet, C.; Seifert, F.M.; Strozzi, T.; Wegmüller, U.; Wieczorek, M.; Wiesmann, A. (2020): ESA Permafrost Climate Change Initiative (Permafrost_cci): Permafrost active layer thickness for the Northern Hemisphere, v2.0. Centre for Environmental Data Analysis, *02 November 2020*. doi:10.5285/29c4af5986ba4b9c8a3cfc33ca8d7c85. http://dx.doi.org/10.5285/29c4af5986ba4b9c8a3cfc33ca8d7c85

ESA CCI+ Permafrost_cci CRDP_v2 (file version 3 1997-2019)

Obu, J.; Westermann, S.; Barboux, C.; Bartsch, A.; Delaloye, R.; Grosse, G.; Heim, B.; Hugelius, G.; Irrgang, A.; Kääb, A.M.; Kroisleitner, C.; Matthes, H.; Nitze, I.; Pellet, C.; Seifert, F.M.; Strozzi, T.; Wegmüller, U.; Wieczorek, M.; Wiesmann, A. (2021): ESA Permafrost Climate Change Initiative (Permafrost_cci): Permafrost active layer thickness for the Northern Hemisphere, v3.0. NERC EDS Centre for Environmental Data Analysis, *28 June 2021*. doi:10.5285/67a3f8c8dc914ef99f7f08eb0d997e23. https://dx.doi.org/10.5285/67a3f8c8dc914ef99f7f08eb0d997e23

5 PERMAFROST EXTENT

5.1 Terminology

The boundary of permafrost can be defined as
1. The geographical boundary between the continuous and discontinuous permafrost zones.
2. The margin of a discrete body of permafrost.
A permafrost region is commonly subdivided into permafrost zones based on the proportion of the ground that is perennially cryotic. The basic subdivision in high latitudes is into zones of continuous permafrost and discontinuous permafrost.
REFERENCES: Muller, 1943; Brown, 1967, 1978; Washburn, 1979; Pewe, 1983.

Continuous permafrost is the major subdivision of a permafrost region in which permafrost occurs everywhere beneath the exposed land surface with the exception of widely scattered sites.
Taliks associated with rivers and lakes may occur in the continuous permafrost zone.
REFERENCE: Brown, 1970.

Discontinuous permafrost corresponds to permafrost occurring in some areas beneath the exposed land surface throughout a geographic region where other areas are free of permafrost.
Discontinuous permafrost occurs between the continuous permafrost zone and the southern latitudinal limit of permafrost in lowlands. Depending on the scale of mapping, several subzones can often be distinguished, based on the percentage (or fraction) of the land surface underlain by permafrost, as shown in the following table.

Permafrost	English usage	Russian Usage
Extensive	65-90%	Massive Island
Intermediate	35-65%	Island
Sporadic	10-35%	Sporadic
Isolated Patches	0-10%	-

5.2 Abstract of data publication

This dataset contains permafrost extent data produced as part of the European Space Agency's (ESA) Climate Change Initiative (CCI) Permafrost project. It forms part of the second version of their Climate Research Data Package (CRDP v3). It is derived from a thermal model driven and constrained by satellite data. Grid products of CDRP v3 are released in annual files, covering the start to the end of the Julian year. This corresponds to average annual ground temperatures (at 2 m depth) which forms the basis for the retrieval of yearly fraction of permafrost-underlain and permafrost-free area within a pixel. A classification according to the IPA (International Permafrost Association) zonation delivers the well-known permafrost zones, distinguishing isolated (0-10%) sporadic (10-50%), discontinuous (50-90%) and continuous permafrost (90-100%).

Case A: It covers the Northern Hemisphere (north of 30°) for the period 2003-2021 based on MODIS Land Surface temperature merged with downscaled ERA5 reanalysis near-surface air temperature data.

Case B: It covers the Northern Hemisphere (north of 30°) for the period 1997-2002 based on downscaled ERA5 reanalysis near-surface air temperature data which are bias-corrected with the Case A product for the overlap period 2003-2021 using a pixel-specific statistics for each day of the year.

5.3 Pixel attributes

Layer	Attribute	Units	Data type	notes
1	Permafrost fraction	percent	integer	yearly fraction of permafrost-underlain and permafrost-free area within a pixel

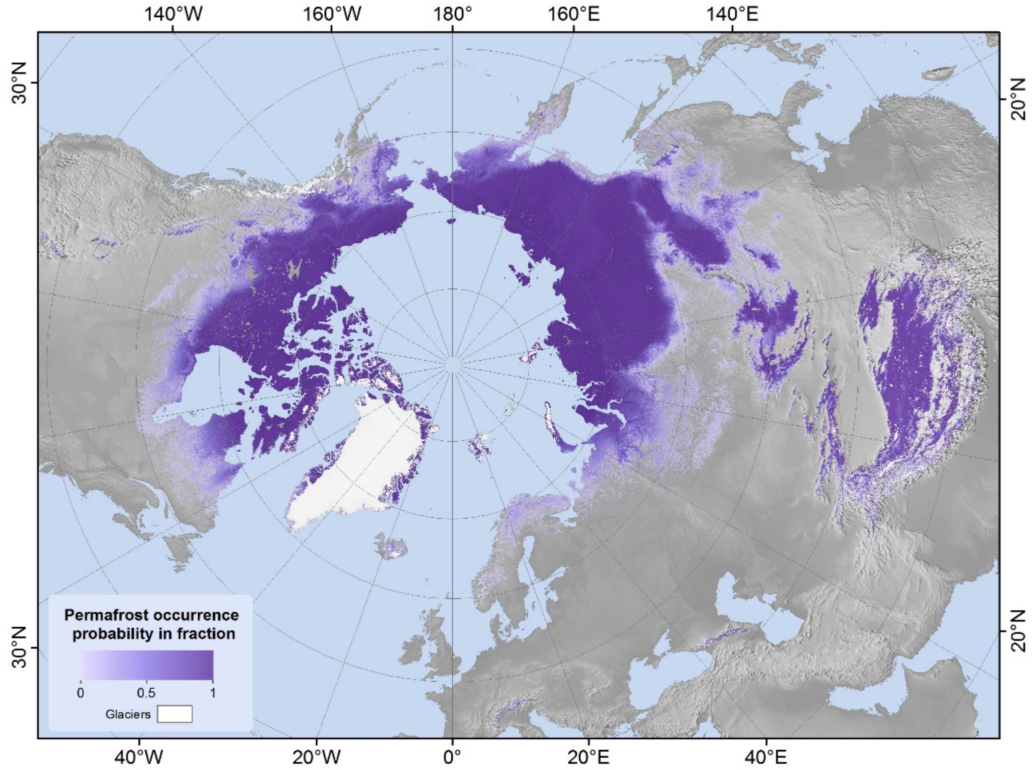

Figure 4: Example of Permafrost extent (fraction) for 2015

5.4 Previous versions

ESA DUE GlobPermafrost (average for 2000-2017; equilibrium model approach; northern hemisphere, Andes, New Zealand, East African Plateau and Antarctic)

Obu, Jaroslav; Westermann, Sebastian; Kääb, Andreas; Bartsch, Annett (2018): Ground Temperature Map, 2000-2016, Northern Hemisphere Permafrost. Alfred Wegener Institute, Helmholtz Centre for Polar and Marine Research, Bremerhaven, PANGAEA, https://doi.org/10.1594/PANGAEA.888600

Obu, Jaroslav; Westermann, Sebastian; Kääb, Andreas; Bartsch, Annett (2019): Ground Temperature Map, 2000-2017, Antarctic. University of Oslo, PANGAEA, https://doi.org/10.1594/PANGAEA.902576

Obu, Jaroslav; Westermann, Sebastian; Kääb, Andreas; Bartsch, Annett (2019): Ground Temperature Map, 2000-2016, Andes, New Zealand and East African Plateau Permafrost. University of Oslo, PANGAEA, https://doi.org/10.1594/PANGAEA.905512

ESA CCI+ Permafrost_cci CRDP_v0 (file version 1 2003-2017)

Obu, J.; Westermann, S.; Barboux, C.; Bartsch, A.; Delaloye, R.; Grosse, G.; Heim, B.; Hugelius, G.; Irrgang, A.; Kääb, A.M.; Kroisleitner, C.; Matthes, H.; Nitze, I.; Pellet, C.; Seifert, F.M.; Strozzi, T.; Wegmüller, U.; Wieczorek, M.; Wiesmann, A. (2019): ESA Permafrost Climate Change Initiative (Permafrost_cci): Permafrost Extent for the Northern Hemisphere, v1.0. Centre for Environmental Data Analysis, *19 December 2019*. doi:10.5285/c7590fe40d8e44169d511c70a60ccbcc. http://dx.doi.org/10.5285/c7590fe40d8e44169d511c70a60ccbcc

ESA CCI+ Permafrost_cci CRDP_v1 (file version 2 1997-2018)

Obu, J.; Westermann, S.; Barboux, C.; Bartsch, A.; Delaloye, R.; Grosse, G.; Heim, B.; Hugelius, G.; Irrgang, A.; Kääb, A.M.; Kroisleitner, C.; Matthes, H.; Nitze, I.; Pellet, C.; Seifert, F.M.; Strozzi, T.; Wegmüller, U.; Wieczorek, M.; Wiesmann, A. (2020): ESA Permafrost Climate Change Initiative (Permafrost_cci): Permafrost extent for the Northern Hemisphere, v2.0. Centre for Environmental Data Analysis, *02 November 2020*. doi:10.5285/28e889210f884b469d7168fde4b4e54f. http://dx.doi.org/10.5285/28e889210f884b469d7168fde4b4e54f

ESA CCI+ Permafrost_cci CRDP_v2 (file version 3 1997-2019)

Obu, J.; Westermann, S.; Barboux, C.; Bartsch, A.; Delaloye, R.; Grosse, G.; Heim, B.; Hugelius, G.; Irrgang, A.; Kääb, A.M.; Kroisleitner, C.; Matthes, H.; Nitze, I.; Pellet, C.; Seifert, F.M.; Strozzi, T.; Wegmüller, U.; Wieczorek, M.; Wiesmann, A. (2021): ESA Permafrost Climate Change Initiative (Permafrost_cci): Permafrost extent for the Northern Hemisphere, v3.0. NERC EDS Centre for Environmental Data Analysis, *28 June 2021*. doi:10.5285/6e2091cb0c8b4106921b63cd5357c97c. https://dx.doi.org/10.5285/6e2091cb0c8b4106921b63cd5357c97c

6 PRODUCT EVALUATION SUMMARY

Evaluation of CRDPv3 is provided in the Product Validation and Intercomparison Report (PVIR) version 4 [RD-2]. Permafrost_cci GTD match-up evaluation shows a median bias of -0.89 °C (mean bias -0.73 °C) for the circum-arctic for the bulk ground temperature data collection spanning depths from the surface down to 10 m and permafrost temperature regimes as well as warmer non-permafrost temperature. In summary, the Permafrost_cci permafrost temperature (that we define as GTD < 1°C) shows good performance with a median bias of 0.35 °C for all depth layers. Users of Permafrost_cci GTD products should consider that Permafrost_cci GTD > 1 °C outside of the permafrost zones is characterized by a cold median MAGT bias of -1.17 °C (mean bias -1.11 °C). This leads in turn to and an overestimation of the areal extent of permafrost (especially in the Permafrost_cci PFR= 29 % class) at the southern boundaries of Permafrost in discontinuous, and sporadic permafrost regions. We consider Permafrost_cci GTD and PFR products for the Northern hemisphere to be most reliable in the permafrost temperature range with GTD < 1 °C and in PFR > 50% as well as PFR <= 29% is reliable as non-permafrost.

Permafrost_cci ALT performance with match-up pairs from China and Mongolia excluded is characterised by a median bias of -13cm (95% CI: -90 to 48 cm) with a robust temporal stability around 60 %. A larger bias > 1 m occurs only in a few match-up pairs in Alaska, Canada and Russia and Permafrost_cci bias < -1.5 m mainly occurs in Svalbard.

PERMOS investigations in the Swiss Alps shows that the performance of Permafrost_cci GTD and Permafrost_cci PFR highly improved for mountain regions. Permafrost_cci GTD shows a slight cold bias of -0.265°C only. At larger depth, Permafrost_cci GTD shows a slight warm bias of +0.275°C at 10 m depth. Due to the major improvement in Permafrost_cci GTD, also the Permafrost_cci PFR product now matches the majority of inventoried ESA GlobPermafrost slope movement products and Permafrost_cci rock glacier products that were located outside of the Permafrost_cci PFR before.

GCOS requirements remain to date undefined for spatially continuous products (see summary in Bartsch et al. 2023 and [RD-5]). Only in situ point measurements are considered for the permafrost ECVs ground temperature and active layer thickness. Permafrost extent is not considered as an ECV but requested according to WMO OSCAR.

7 APPLICATION EXAMPLES

7.1 Climate model assessment

In order to assess the impact of the boundary parameters for vegetation and soil in the coupled model HIRHAM-CLM on representation of the cryosphere and atmosphere, nine different model runs have been conducted and evaluated them against in situ measurements and remote sensing based data products from CCI+ Permafrost [RD-4]. The model was run from 1979-2019 with lower and lateral boundary forcing from the ERA5 reanalysis. In summary, changing boundary parameters for land has significantly impacted soil temperatures in our model runs. Using all boundary parameters derived from CCI Landcover and CCI Permafrost improved not only the representation of soil temperature but also the representation of air temperature.

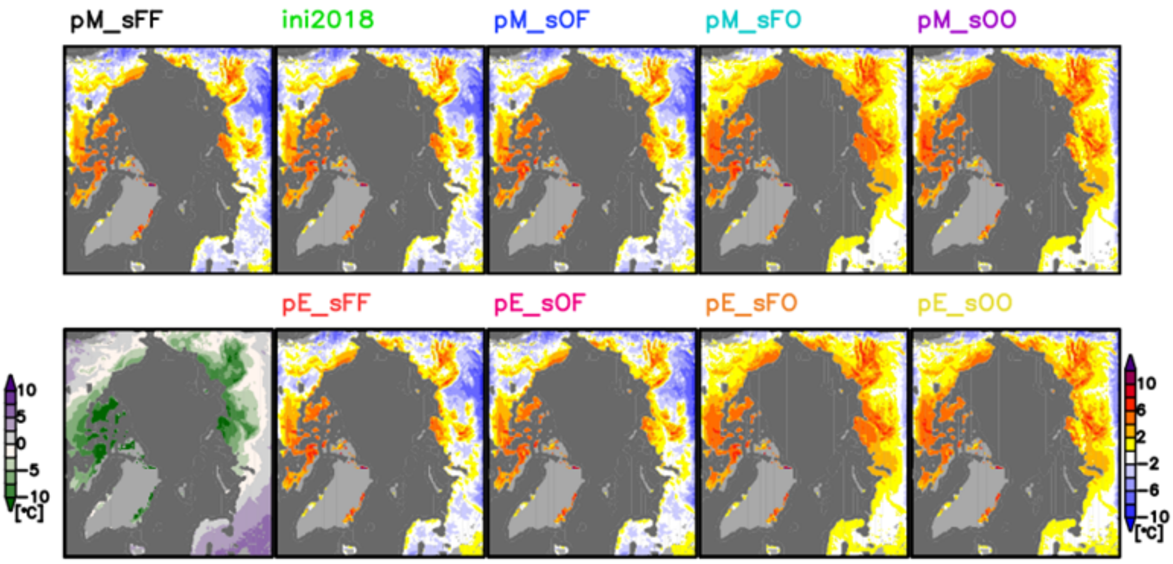

Figure 5: Mean annual ground temperature at 1m depth, averaged over 2003-2019, from CCI+ Permafrost product (lower left panel) and difference to HIRHAM-CLM model runs (model run minus CCI+Permafrost). For abbreviations see [RD-4].

7.2 Comparison of ALT to landcover trends: example fire scars

The relation between net lake area loss of shrinking lakes (negative net lake change) from the HRPC lake change datasets (Nitze et al., 2018) has been analysed for four continental scale permafrost transects [RD-4]. The HRPC contains information on Landsat-based trends of landscape disturbances, which may trigger changes in the ground thermal regime or become enhanced by regional to local changes in ground thermal regime. In all sites, ALT was larger for burned sites than for non-burned sites, which can be expected as wildfires predominantly occur in warmer, forested boreal sites.

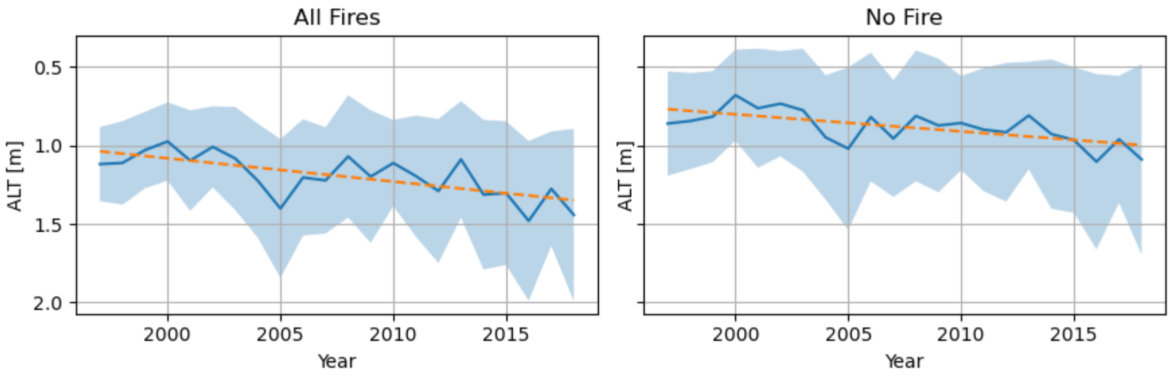

Figure 6: Mean (line), standard deviation (shading) and trend of mean (orange dashed line) of modelled active layer thickness (ALT) in burned and unburned regions in Transect T3 Alaska. (for details see [RD-4]).

7.3 Comparison of ground temperature to coastal erosion

In order to assess SAR applicability for coastal erosion quantification, data acquired at L-band has been investigated and compared to Landsat based retrievals. The derived rates suggest an increase of erosion at all study sites in recent years (Figure 7) but uncertainties are also high. However, CRDPv0 ground temperatures at 2 m depth have also been increasing at all these sites between 2003-2017.

	Rate from GlobPermafrost trend product 1999-2014	Rate from L-band SAR 2007-2018	Previously published rates
Varandai (c)	n.a.	-5.41 ± 2.64	-1.8 (1951-2013) [1]
Herschel (B)	-4.19 ± 2.8	-7.02 ± 2.65	-6.8 (2012-2013) [2]
Kay Point (B)	-3.94 ± 1.4	-5.90 ± 0.41	-1.7 (1990-2011) [3]
Bykosvky (D)	-5.83 ± 2.8	-4.81 ± 1.37	-1 - -2 (1951-2006) [4]

(1) Sinistyn et al. 2019, (2) Obu et al. 2016, (3) Irrgang et al. 2017, (4) Lantuit et al. 2011

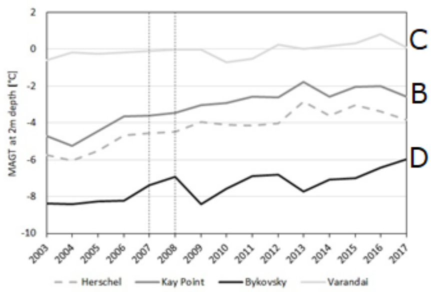

Figure 7: Erosion rate retrieval summary from Bartsch et al. (2020). Most sites show increased recent rates (left) as well as increasing ground temperatures (right, source CRDPv0). GlobPermafrost product: Landsat based rates. L-band SAR: PALSAR and PALSAR2.

7.4 Cross ECV assessment – sea ice extent

Ground temperature increase at 2 m depth is highest along the Arctic coastline (Miner et al. 2022). The overall trend for the northern hemisphere follows sea ice decline (R^2= 0.75; Bartsch et al. 2023). The lower the minimum sea ice extent, the higher the temperatures in the ground (Figure 8). A change of on average one degree Celsius at 2 m depth (referring to the area of permafrost extent maximum within the observation period for CRDPv2, 1997–2019) coincides with a September sea ice decline of about 2.5 million km^2.

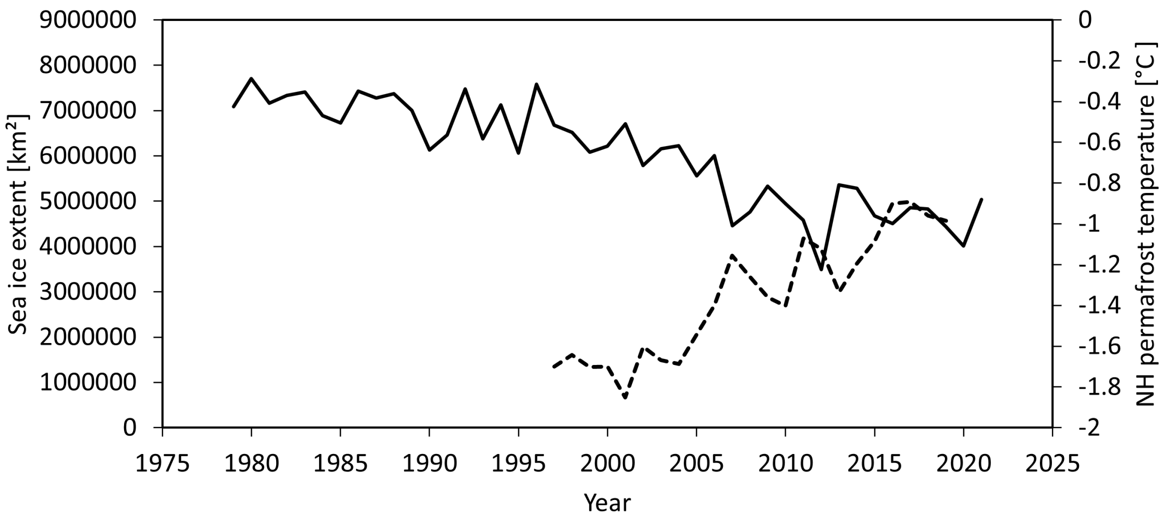

*Figure 8: Northern hemisphere (NH) permafrost temperature change at 2 m depth (dashed line; source transient modelling using landsurface temperature (reanalyses data and near infrared (MODIS, 1 km); CryoGRID; Permafrost_cci v*3 (CRDPv2)*, compared to sea ice extent for September (solid line; sea ice concentration data from 1979 to 2021 were obtained from https:// www. meere ispor tal. de (grant: REKLIM-2013-04, Spreen et al. (2008)). Source:* B*artsch et al. (2023).*

7.5 Settlements at risk – permafrost extent, ground temperature and active layer thickness trends extrapolation to 2050

A first panarctic satellite-based record of expanding infrastructure and anthropogenic impacts along all permafrost affected coasts (100 km buffer, ≈6.2 Mio km2), named the Sentinel-1/2 derived Arctic Coastal Human Impact (SACHI) dataset has been recently published (Bartsch et al. 2021b). It has been combined with Permafrost_cci CRDPv2. Trends have been derived and extrapolated for infrastructure objects across the Arctic. 55% of the identified human impacted area will be shifting to above 0 ◦C ground temperature at two meter depth by 2050 if current permafrost warming trends continue at the pace of the last two decades, highlighting the critical importance to better understand how much and where Arctic infrastructure may become threatened by permafrost thaw.

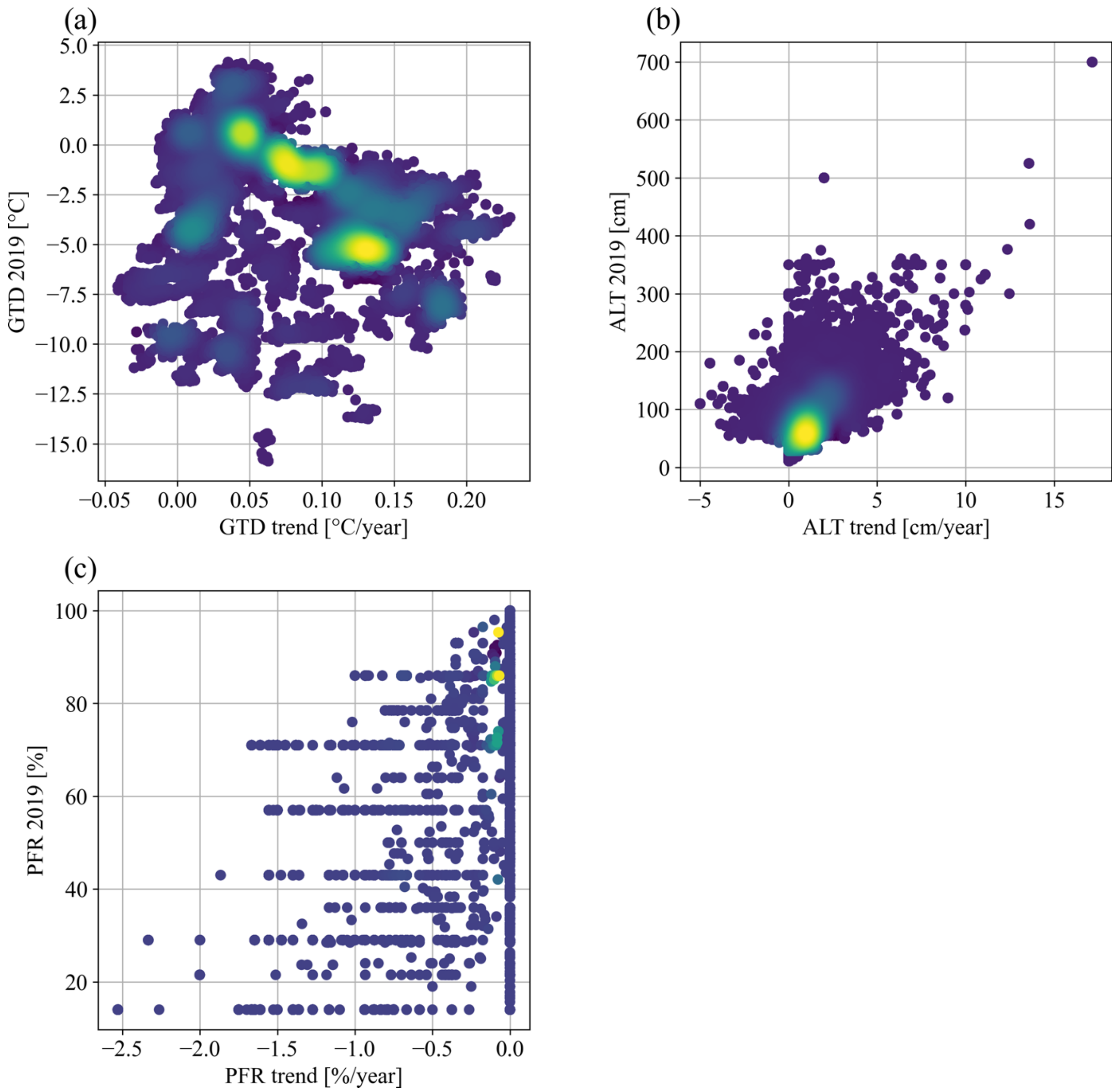

Figure 9: Scatterplots of trend versus 2019 status for a) Ground temperature at 2 m depth, b) Active layer thickness and c) Permafrost fraction. Each point represents the average for a distinct object within human impacted areas as mapped with Sentinel-1and -2 . Calculations are based on CRDPv2. Source: Bartsch et al. (2021)

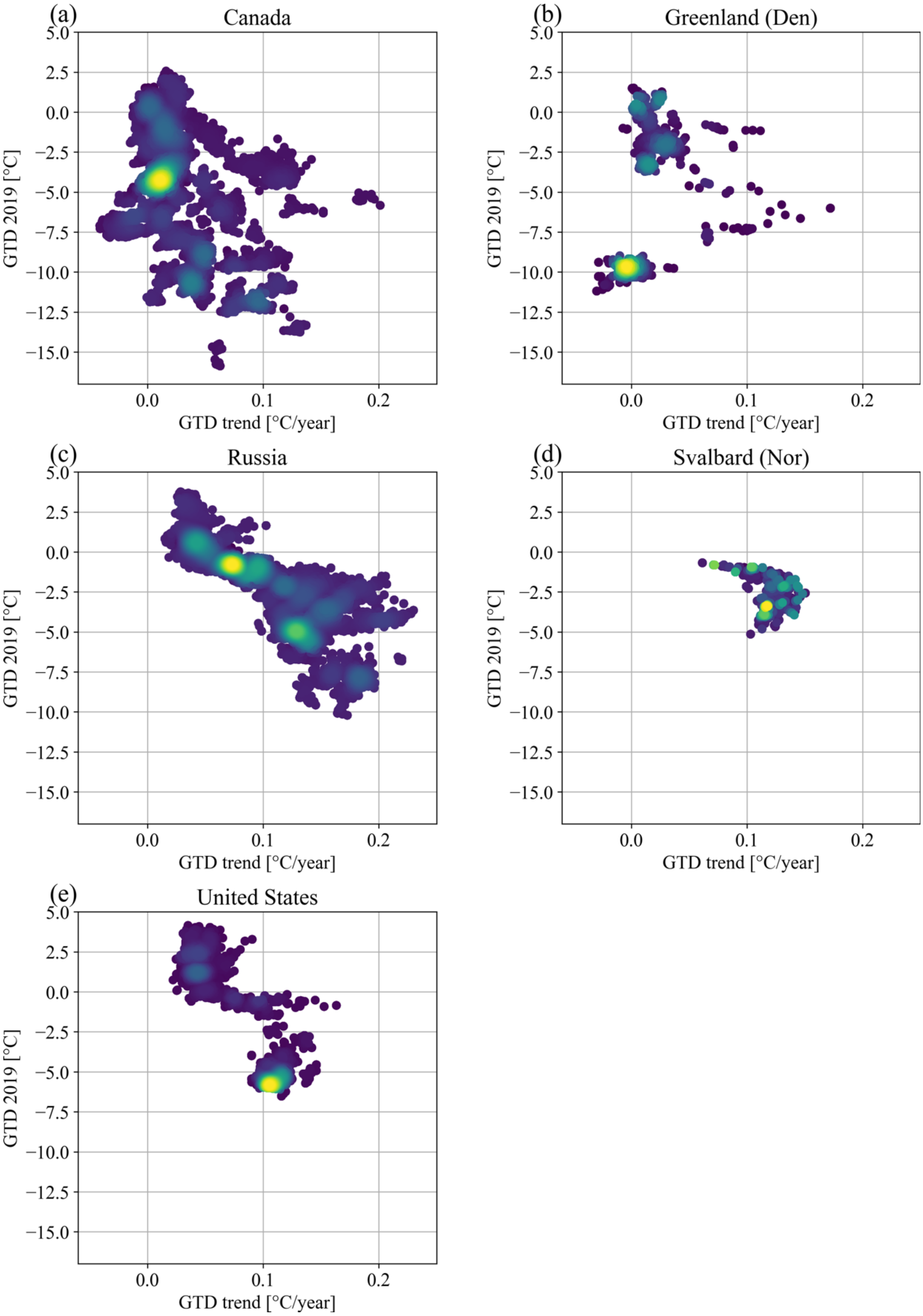

Figure 10: Scatterplots of trend versus 2019 status for Ground temperature at 2 m depth separated by region. Each point represents the average for a distinct object within human impacted areas as mapped with Sentinel-1 and -2. Calculations are based on CRDPv2. Modified from Bartsch et al. (2021)

8 KNOWN LIMITATIONS

The active layer thickness is strongly dependent on the employed ground stratigraphy. As ground stratigraphies are known to vary on short distances, the performance of the active layer thickness product strongly varies in space, being less accurate especially where ground stratigraphies are incorrect. This can lead to deviations of several meters in extreme cases.

9 REFERENCES AND ACRONYMS

9.1 Applicable documents

[AD-1] ESA 2017: Climate Change Initiative Extension (CCI+) Phase 1 – New Essential Climate Variables - Statement of Work. ESA-CCI-PRGM-EOPS-SW-17-0032

[AD-2] Requirements for monitoring of permafrost in polar regions - A community white paper in response to the WMO Polar Space Task Group (PSTG), Version 4, 2014-10-09. Austrian Polar Research Institute, Vienna, Austria, 20 pp

[AD-3] ECV 9 Permafrost: assessment report on available methodological standards and guides, 1 Nov 2009, GTOS-62

[AD-4] GCOS-200, the Global Observing System for Climate: Implementation Needs (2016 GCOS Implementation Plan, 2015.

[AD-5] ESA Climate Office 2020: CCI Data Standards v2.2. Reference CCI-PRGM-EOPS-TN-13-0009

9.2 Reference Documents

[RD-1] Bartsch, A., Westermann, Strozzi, T., Wiesmann, A., Kroisleitner, C., Wiesczorek, M., Heim B. (2023): ESA CCI+ Permafrost Product Specifications Document, v4.0

[RD-2] Heim, B., Wieczorek, M., Pellet, C., Delaloye, R., Bartsch, A., Strozzi, T. (2024): ESA CCI+ Permafrost Product Validation and Intercomparison Report, v4.0

[RD-3] Westermann, S., Bartsch, A., Strozzi, T. (2023): ESA CCI+ ATBD, v4.0

[RD-4] Bartsch, A., Nitze, I., Grosse, G., Heim, B., Wieczorek, M., Matthes, H., Bartsch, A., Strozzi, T., Lisovski, S. (2022): ESA CCI+ Climate Assessment Report, v3.0

[RD-5] Bartsch, A., Matthes, H., Westermann, S., Heim, B., Pellet, C., Onacu, A., Kroisleitner, C., Strozzi, T. (2023): ESA CCI+ Permafrost User Requirements Document, v3.0

9.3 Bibliography

Bartsch, A., Ley, S., Nitze, I., Pointner, G., & Vieira, G. (2020). Feasibility study for the application of Synthetic Aperture Radar for coastal erosion rate quantification across the Arctic. Frontiers in Environmental Science, 8(143). https://doi.org/10.3389/fenvs.2020.00143

Bartsch, A., Strozzi, T., and Nitze, I.: Permafrost Monitoring from Space, Surveys in Geophysics, 2023.
https://link.springer.com/article/10.1007/s10712-023-09770-3

Bartsch, A., G. Pointner, I. Nitze, A. Efimova, D. Jakober, S. Ley, E. Högström, G. Grosse, P. Schweitzer (2021): Expanding infrastructure and growing anthropogenic impacts along Arctic coasts. *Environmental Research Letters*. https://doi.org/10.1088/1748-9326/ac3176

Brown R.J.E., 1967: Permafrost Map of Canada. National Research Council Canada, Pub. NRC 9769 and Geological Survey of Canada, Map 1246A (with marginal notes)

Brown R.J.E., 1970: Permafrost in Canada: Its influence on northern development. University of Toronto Press, Toronto 234 p.

Brown R.J.E., 1978: Permafrost Map of Canada. In: Hydrological Atlas of Canada, Department of Fisheries and Environment, Ottawa, Canada, Plate No. 32.

Miner, K.R., Turetsky, M.R., Malina, E., Bartsch, A., Tamminen, J., McGuire A.D., Fix, A., Sweeney, C., Elder, C.D., Miller, C.E (2022). Permafrost carbon emissions in a changing Arctic. *Nat Rev Earth Environ* 3, 55–67. https://doi.org/10.1038/s43017-021-00230-3

Muller S.W, 1943: Permafrost or permanently frozen ground and related engineering problems. U.S. Engineers Office, Strategic Engineering Study, Special Report No. 62. 136p. (Reprinted in 1947, J. W. Edwards, Ann Arbor, Michigan, 231p.)

Nitze I, Grosse G, Jones BM, Romanovsky VE, Boike J (2018) Remote sensing quantifies widespread abundance of permafrost region disturbances across the Arctic and Subarctic. Nat Commun 9(1):5423. https:// doi. org/ 10. 1038/ s41467- 018- 07663-3

Obu J., S. Westermann, A. Bartsch, N. Berdnikov, H. H. Christiansen, A. Dashtseren, R. Delaloye, B. Elberling, B. Etzelmüller, A. Kholodov, A. Khomutov, A. Kääb, M. O. Leibman, A. G. Lewkowicz, S. K. Panda, V. Romanovsky, R. G. Way, A. Westergaard-Nielsen, T. Wu, J. Yamkhin, D. Zou (2019): Northern Hemisphere permafrost map based on TTOP modelling for 2000-2016 at 1 km2 scale. Earth-Science Reviews, 193, 299-316.

Péwé T.L., 1983: Alpine permafrost in the contiguous United States: A review, Arctic and Alpine Research, Vol. 15, No.2, pp. 145-156

van Everdingen R.O., 1985: Unfrozen permafrost and other taliks. Workshop on Permafrost Geophysics, Golden, Colorado, October 1984 (J. Brown, M.C. Metz, P. Hoekstra, Editors). U.S. Army, C.R.R.E.L., Hanover, New Hampshire, Special Report 85-5, pp.101-105 van Everdingen, Robert, ed. 1998 revised May 2005. Multi-language glossary of permafrost and related ground-ice terms. Boulder, CO: National Snow and Ice Data Center/World Data Center for Glaciology. (http://nsidc.org/fgdc/glossary/; accessed 23.09.2009)

Washburn, A.L., 1973: Periglacial processes and environments. Edward Arnold, London, 320p.

Washburn, A. L., 1979: Geocryology. Edward Arnold, London, 406p.

Williams, J.R., 1965: Ground water in permafrost regions: An annotated bibliography. U.S. Geological Survey, Professional Paper 696, 83p.

9.4 Acronyms

ACOP	Asian Conference on Permafrost
ALT	Active Layer Thickness
Arctic CORDEX	Coordinated Regional Climate Downscaling Experiment
AWI	Alfred Wegener Institute Helmholtz Centre for Polar and Marine Research
B.GEOS	b.geos GmbH
CALM	Circumpolar Active Layer Monitoring
CliC	Climate and Cryosphere project
CLM4	Land Community Model
CCI	Climate Change Initiative
CMIP-6	The Coupled Model Intercomparison Project
CMUG	Climate Modelling User Group
CRESCENDO	Coordinated Research in Earth Systems and Climate: Experiments, Knowledge, Dissemination and Outreach
CRG	Climate Research Group
ECV	Essential Climate Variable
EO	Earth Observation
ESA	European Space Agency
ESA DUE	ESA Data User Element
GAMMA	Gamma Remote Sensing AG
GCOS	Global Climate Observing System
GCW	Global Cryosphere Watch
GT	Ground Temperature
GTN-P	Global Terrestrial Network for Permafrost
GTOS	Global Terrestrial Observing System
GUIO	Department of Geosciences University of Oslo
HIRHAM	High Resolution Limited Area Model
IASC	International Arctic Science Committee
ILAMB	International Land Model Benchmarking
IPA	International Permafrost Association
IPCC	Intergovernmental Panel on Climate Change

LS3MIP	Land Surface, Snow and Soil Moisture
MAGT	Mean Annual Ground Temperature
NetCDF	Network Common Data Format
NSIDC	National Snow and Ice Data Center
PCN	Permafrost Carbon Network
PE	Permafrost Extent
PERMOS	Swiss Permafrost Monitoring Network
PF	Permafrost
PSTG	Polar Space Task Group
RASM	Regional Arctic System Model
RD	Reference Document
RMSE	Root Mean Square Error
RS	Remote Sensing
SAR	Synthetic Aperture Radar
SCAR	Scientific Committee on Antarctic Research
SU	Department of Physical Geography Stockholm University
TSP	Thermal State of Permafrost
UNIFR	Department of Geosciences University of Fribourg
URD	Users Requirement Document
WCRP	World Climate Research Program
WMO	World Meteorological Organisation
WMO OSCAR	Observing Systems Capability Analysis and Review Tool
WUT	West University of Timisoara